Received: 3 January 2022 | Revised: 4 February 2022 | Accepted: 5 February 2022

DOI: 10.1002/pol.20220003

RESEARCH ARTICLE

JOURNAL OF POLYMER SCIENCE WILEY

On-surface synthesis of porous graphene nanoribbons containing nonplanar [14]annulene pores

M. R. Ajayakumar[1] | **Marco Di Giovannantonio**[2] | **Carlo A. Pignedoli**[2] | **Lin Yang**[1] | **Pascal Ruffieux**[2] | **Ji Ma**[1] | **Roman Fasel**[2,3] | **Xinliang Feng**[1,4]

[1]Center for Advancing Electronics Dresden (cfaed), Faculty of Chemistry and Food Chemistry, Technische Universitat Dresden, Dresden, Germany

[2]nanotech@surfaces laboratory, Empa – Swiss Federal Laboratories for Materials Science and Technology, Dübendorf, Switzerland

[3]Department of Chemistry, Biochemistry and Pharmaceutical Sciences, University of Bern, Bern, Switzerland

[4]Department of Synthetic Materials and Functional Devices, Max Planck Institute of Microstructure Physics, Halle, Germany

Correspondence
Ji Ma and Xinliang Feng, Center for Advancing Electronics Dresden, Department of Chemistry and Food Chemistry, Technische Universitat Dresden, Dresden 01062, Germany.
Email: ji.ma@tu-dresden.de and xinliang.feng@tu-dresden.de

Roman Fasel, Empa, Swiss Federal Laboratories for Materials Science and Technology, Dübendorf 8600, Switzerland.
Email: roman.fasel@empa.ch

Present address
Marco Di Giovannantonio, Istituto di Struttura della Materia–CNR (ISM-CNR), Rome, Italy

Funding information
Swiss Supercomputing Center, Grant/Award Number: s904; TU Dresden; Swiss National Science Foundation, Grant/Award Number: 200020_182015; DFG-SNSF Joint Swiss-German Research Project, Grant/Award Numbers: 200020_187617, 429265950; Center for Advancing Electronics Dresden; ERC Consolidator Grant, Grant/Award Number: 819698; EU Graphene Flagship, Grant/Award Number: 881603

Abstract

The precise introduction of nonplanar pores in the backbone of graphene nanoribbon represents a great challenge. Here, we explore a synthetic strategy toward the preparation of nonplanar porous graphene nanoribbon from a predesigned dibromohexabenzotetracene monomer bearing four cove-edges. Successive thermal annealing steps of the monomers indicate that the dehalogenative aryl-aryl homocoupling yields a twisted polymer precursor on a gold surface and the subsequent cyclodehydrogenation leads to a defective porous graphene nanoribbon containing nonplanar [14]annulene pores and five-membered rings as characterized by scanning tunneling microscopy and noncontact atomic force microscopy. Although the C–C bonds producing [14]annulene pores are not achieved with high yield, our results provide new synthetic perspectives for the on-surface growth of nonplanar porous graphene nanoribbons.

KEYWORDS

cove-edge, five-membered ring, graphene nanoribbon, nanopore, nonplanar, on-surface synthesis

M. R. Ajayakumar and Marco Di Giovannantonio contributed equally to this study.

1 | INTRODUCTION

Porous graphene nanostructures have recently attracted much attention due to their potential as active components in a variety of applications, including water desalination, gas separation, ion transport and sensing.[1] Since their electronic properties and functionalities are sensitively related to size, location, density and shape of the pores, it is desirable to develop efficient strategies to create well-defined nanoscale pores in graphene nanostructures. In contrast to the top-down methods using an oxygen plasma[1] or ultraviolet-induced oxidative etching[2] on graphene, the combination of in-solution and on-surface syntheses represents a unique approach for the construction of atomically defined pores in graphene nanostructures. For example, this strategy has recently enabled the synthesis of nanoporous graphene networks[3] and nanoporous nanoribbons[4] with different pore sizes associated with unique electronic properties. In addition to the tailored pore size, the conformation of the pores in graphene nanostructures also plays an important role to tailor their electronic and mechanical properties.[1,5] Depending on the inner edge structure, the nanopore can have either planar or nonplanar geometry (Figure 1A)[6]; for instance, the creation of one "benzene" vacancy in graphene nanostructure leads to a planar 18-membered pore (or [18]annulene, (a), while the exclusion of one "C-C bond" creates a nonplanar 14-membered pore (or [14]annulene, (b). The latter type of pores has been recently reported by our group,[7] with the introduction of three nonplanar [14]annulene pores into a graphene molecule via on-surface cyclodehydrogenation of a propeller molecular precursor with 78 sp^2 carbon atoms, which exhibits an enlarged energy gap in comparison to its planar non-porous counterpart with 84 sp^2 carbon atoms. Peña and Godlewski et al.[8] also synthesized a large trigonal porous nanographene with 102 sp^2 carbon atoms by using a similar strategy and explored the reactivity of the nonplanar [14]annulene pores on a gold surface. However, the incorporation of nonplanar pores into the backbone of graphene nanoribbons has remained less investigated, mostly due to the lack of suitable precursor designs.

In this work, we demonstrate the combined in-solution and on-surface synthesis of porous graphene nanoribbon with nonplanar [14]annulene pores on a coinage metal surface under ultrahigh vacuum (UHV) conditions. Conceptually, the targeted nonplanar porous GNR (nPGNR) can be exemplified by the periodic removal of C-C bonds in the backbone of an armchair-edged GNR of width $N = 11$ (11-AGNR) along the ribbon longitudinal axis (Figure 1B). The calculated density of states (DOS) and band structure of the nPGNR reveal a significantly increased bandgap of 1.66 eV (Figure 1C), compared to the pristine non-porous 11-AGNR (0.15 eV).[6] As illustrated in Figure 1B, a new building block with four cove-edges, that is, 10,21-dibromohexabenzo[*a*,*c*,*fg*,*j*,*l*,*op*]tetracene (DBHBT, **1**), is designed and synthesized via wet chemistry methods. This DBHBT precursor is expected to provide

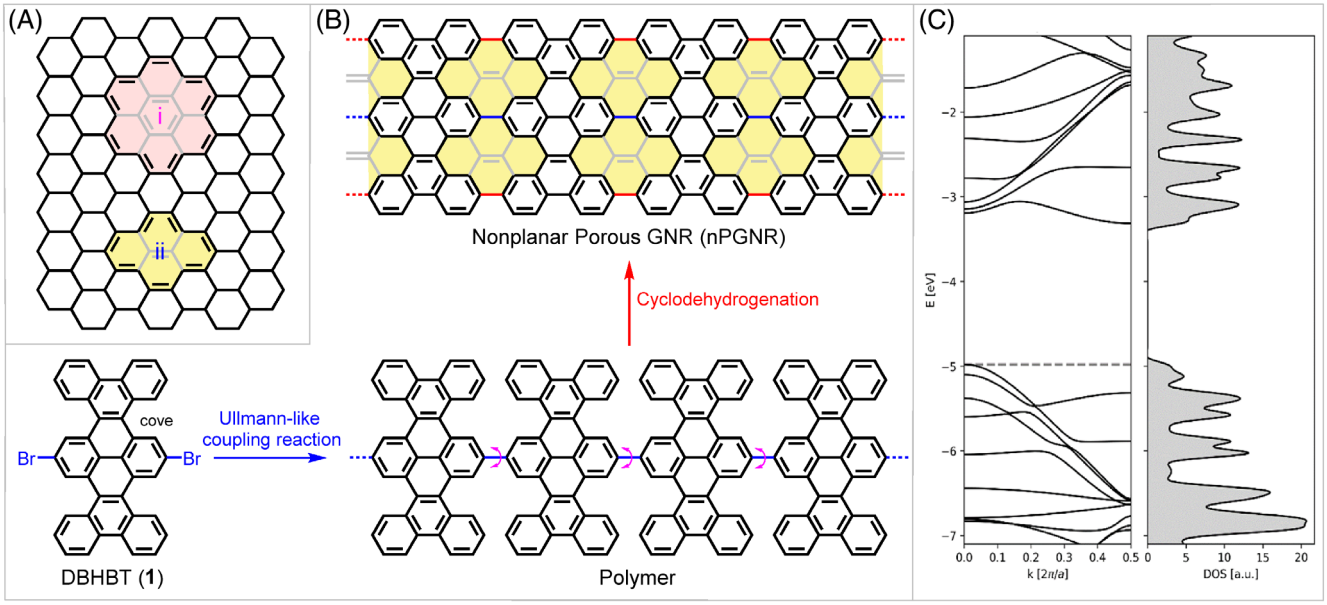

FIGURE 1 (A) Examples of planar (i) and nonplanar (ii) pores in graphene nanostructures; (B) Conceptual on-surface synthesis of nPGNR (pink arrows indicate the rotational freedom of each unit around the newly formed bonds); (C) Band structure and DOS of the targeted nPGNR with a band gap of 1.66 eV. The gray dashed line indicates the top of the valence band

the targeted nPGNR through the surface-assisted Ullmann-like coupling and subsequent cyclodehydrogenation reaction. Upon annealing of DBHBT monomers deposited on Au(111), the monomers smoothly undergo the dehalogenative aryl-aryl coupling in the first step to afford the expected polymers at 200°C, as shown by scanning tunneling microscopy (STM) images. However, in the second step under annealing at 400°C, we found that the obtained polymers could not undergo the complete cyclodehydrogenation to form the targeted nPGNR. Instead, a defective GNR containing nonplanar [14]annulene pores and additional five-membered rings is achieved. The chemical structure of the product, including five-membered rings created upon closing some of the cove edges,[8,9] is demonstrated by high-resolution noncontact atomic force microscopy (nc-AFM). Our results provide a novel insight into the design and synthesis of nonplanar porous GNRs.

2 | RESULTS AND DISCUSSION

The synthesis of monomer **1** was carried out in solution as displayed in Scheme 1. First, 2,7-bis(4,4,5,5-tetramethyl-1,3,2-dioxaborolan-2-yl)pyrene (**3**) was prepared using an iridium-catalyzed borylation of the commercially available pyrene (**2**) according to the reported procedure.[10] Subsequently, the key intermediate **5** was synthesized in 17% yield through the twofold annulative π-extension reaction[11] with 5,5-dimethyl-5*H*-dibenzo[*b*,*d*]silole (**4**) in 1,2-dichloroethane at 80 °C in the presence of $Pd(CH_3CN)_4(SbF_6)_2$ catalyst and *o*-chloranil. After that, compound 5 was treated with copper(II) bromide ($CuBr_2$) for 24 h at 95°C to afford the DBHBT (**1**) with a yield of 40%. After purification by column chromatography on silica gel, compound **1** was recrystallized in CH_2Cl_2/MeOH to ensure the high purity required by the on-surface synthesis. The chemical structure of **1** was fully characterized by NMR spectroscopy (Figures S3–S6). High-resolution matrix-assisted laser desorption/ionization-time of flight (MALDI-TOF) mass spectrometry analysis of **1** showed an intense peak at m/z = 657.9941 (positive mode, dithranol as the matrix) with isotopic distribution patterns that matched well with the calculated spectrum (calculated value for $C_{40}H_{20}Br_2^+$: m/z = 657.9932) (Figure S11). In addition, the DFT optimized structure of monomer **1** reveals a nonplanar conformation due to steric repulsion between the C-H bonds at the cove positions (Figure S13). Notably, the benzene rings along the cove edges in **1** adopt a mixed up-down conformation with a largest torsional angle of 33.5°.

To explore the on-surface synthesis of nPGNRs, we deposited the nonplanar cove-edged monomer **1** onto a clean Au(111) surface at room temperature (RT) under UHV conditions. STM investigation of the resulting surface displays intact molecules arranged along chains that follow the underlying herringbone reconstruction of the Au(111) substrate (Figure 2A). Closer inspection of these structures (Figure 2B) reveals rectangular features with two bright protrusions at the center of their long sides, which we assign to bromine atoms still attached to the precursor monomers. Such assembly is most likely stabilized by halogen-hydrogen interactions. To induce dehalogenative aryl-aryl coupling, we annealed the substrate to 200°C. As confirmed in previous studies,[12] this temperature is sufficient to promote debromination on Au(111). As expected, after such temperature treatment we observed the formation of (almost) straight stripes decorated with some bright dots (Figure 2C,D). We assign these nanostructures to polymers, where C–C bonds between the initially brominated sites of the monomers have formed, and where the phenanthrene subunits (or just part of them) are pointing either away from or toward the substrate, in virtue of the rotational freedom of each repeat unit around the newly formed C–C bonds (Figure 1B). Further annealing of the sample to 300°C resulted in a reduced number of bright protrusions (Figure 2E,F), which can be ascribed to local

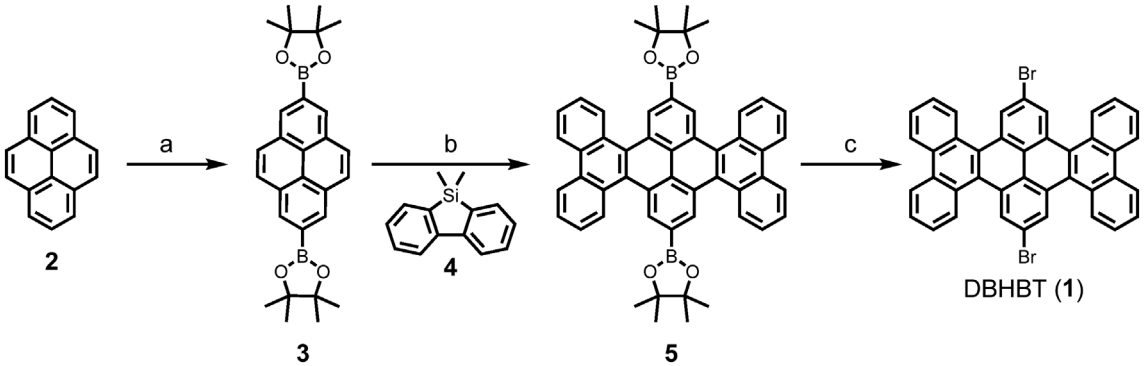

SCHEME 1 Synthetic route to precursor **1**. Reagents and conditions: (a) B_2pin_2, $[Ir(OMe)cod]_2$, dtbpy, cyclohexane, 70°C, 20 h, 65%; (b) $Pd(CH_3CN)_4(SbF_6)_2$, *o*-chloranil, $ClCH_2CH_2Cl$, 80°C, 2 h, 17%; (c) $CuBr_2$, THF/MeOH/H_2O, 95°C, 24 h, 40%

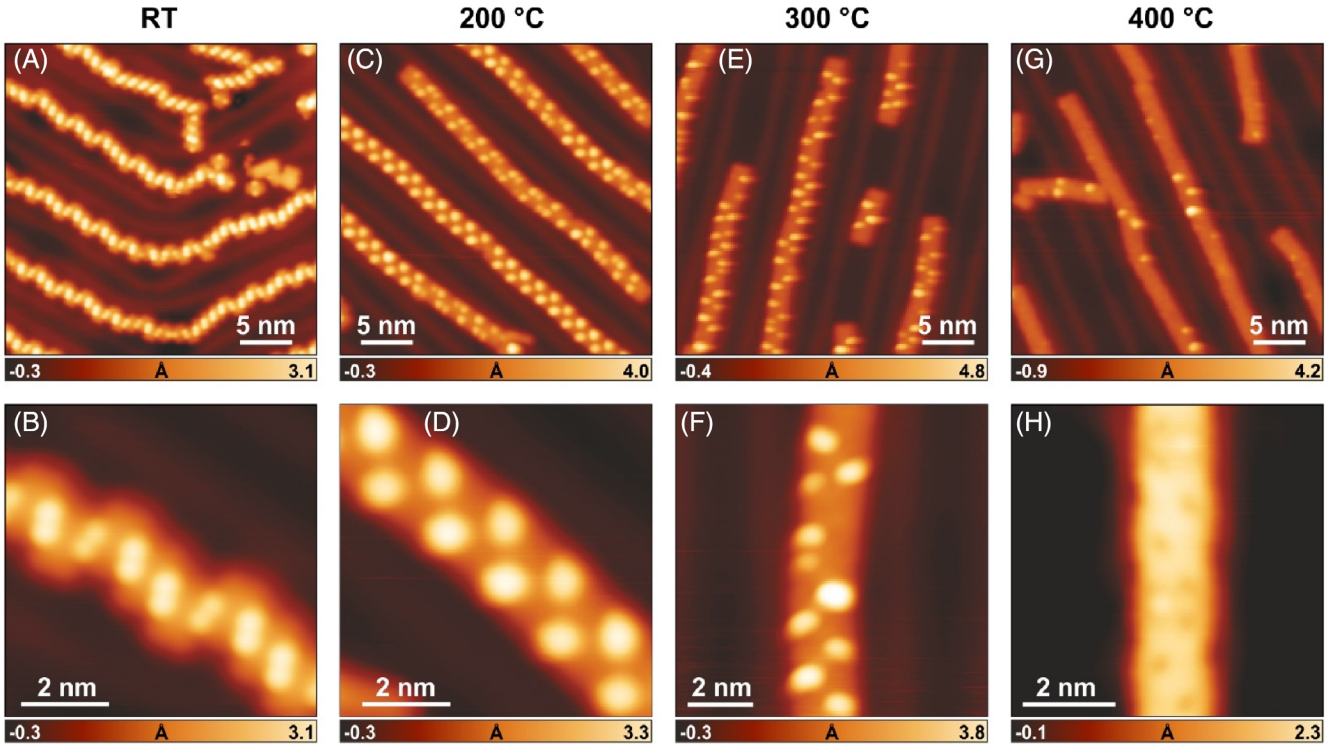

FIGURE 2 STM images of the Au(111) surface after deposition of **1** at RT (A,B) and subsequent annealing to the indicated temperatures (C–H). Scanning parameters: $V_b = -0.7$ V, $I_t = 50$ pA (A,B); $V_b = -1.0$ V, $I_t = 30$ pA (C–G); $V_b = -20$ mV, $I_t = 100$ pA (H)

cyclodehydrogenation processes with the creation of C–C bonds between the phenanthrene subunits of the polymers. This process is almost completed after annealing to 400°C, where only few remaining bright features are left (Figure 2G) and the resulting nanostructures are mostly planar and with some darker sites (Figure 2H).

To get atomically-resolved insights into the obtained nanostructures, we performed constant-height nc-AFM measurements with a CO-functionalized tip of a regular segment obtained after annealing the sample to 420°C (Figure 3). The frequency-shift image reveals that the obtained product is still not completely planar, but entails some distortion. The brighter features at the edges (Figure 3C) are due to six-membered rings pointing away from the surface as a result of steric repulsion of hydrogen atoms facing each other. On the other hand, the opposing six-membered rings are bent toward the surface and appear as faint features in the nc-AFM image. These features are highlighted in the scheme in Figure 3D. Notably, in some cases successful cyclodehydrogenation was achieved between these hexabenzotetracene units, leading to the formation of C–C bonds (red lines in Figure 3D) and consequently nonplanar [14]annulene pores are formed as in the expected structure of the sought-for nPGNR. Unfortunately, the absence of such pore formation in some positions of the ribbon prevented from achieving the desired final nPGNR. However, it is interesting to note that when the pores did not form, cyclodehydrogenation of the inner cove edges led to the formation of five-membered rings (Figure 3C,D), which is also observed in other reported graphene nanostructures containing cove-edges.[8,9] Hence, the darker dots visible in the STM images (Figures 2H and 3A,B) are due to the nonplanar [14]annulene pores, characterized by two opposing hydrogen atoms pointing away from the substrate and the remaining two pointing toward it. It is interesting to note that the bending direction of these hydrogens within the pores is structurally consistent with the overall distortion at the GNR edges, which produces an undulated geometry both in the longitudinal and transverse GNR directions.

3 | CONCLUSIONS

In summary, by combining in-solution and on-surface chemistry, we have synthesized a porous GNR containing nonplanar [14]annulene pores and five-membered rings. The structures of the obtained defective GNR and the corresponding intermediates have been well characterized by means of STM and nc-AFM experiments. The specifically designed precursor DBHBT containing cove-edges allows the surface-assisted Ullmann-like polymerization to afford the expected polymers. However, the subsequent cyclodehydrogenation step finally led to defective porous graphene nanostructures embedding five-membered rings and only a partial amount of 14-membered pores as

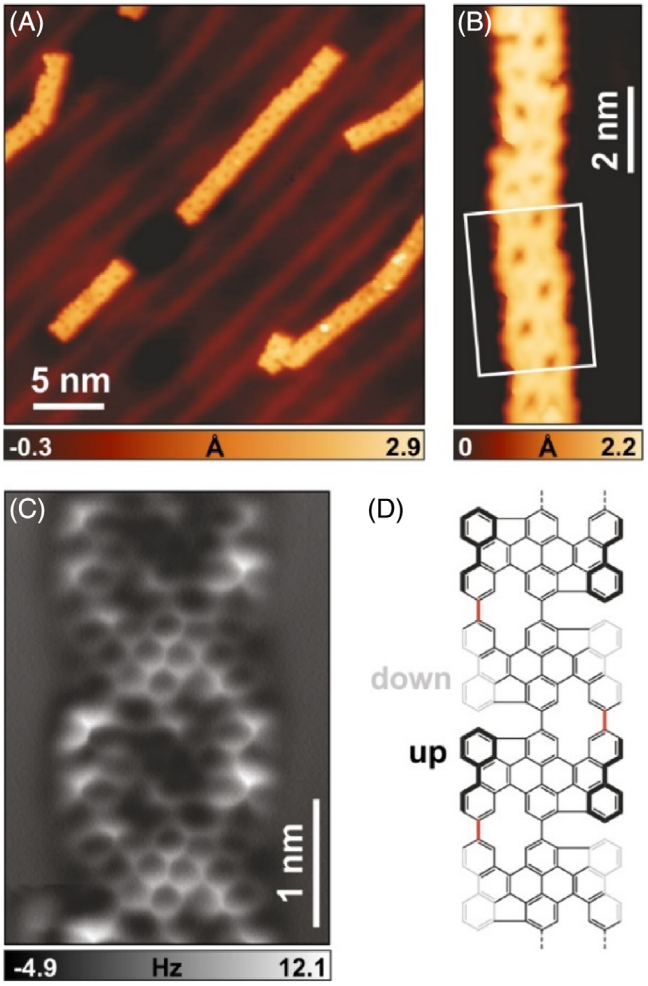

FIGURE 3 Structural investigation of a GNR segment. (A) STM image after deposition of **1** on Au(111) and annealing to 420°C; (B) Zoom-in STM image of a porous GNR; (C) nc-AFM image acquired with a CO-functionalized tip on the GNR segment highlighted in B; (D) Chemical scheme of the structure observed in C. Scanning parameters: $V_b = -0.1$ V, $I_t = 100$ pA (A); $V_b = -20$ mV, $I_t = 100$ pA (B); $\Delta z = +180$ Å with respect to STM set point: $V_b = -5$ mV, $I_t = 100$ pA (C)

compared to the targeted geometry. Although the formation of the anticipated nPGNR is not achieved, the insights reported herein are instructive to the synthesis of other nonplanar porous graphene nanoribbons with high structural perfection.

4 | EXPERIMENTAL SECTION

4.1 | Synthesis and characterizations of precursor 1

All the experimental details for the synthesis of new compounds and precursor 1, and associated characterizations are reported in Supporting information S1.

4.2 | Sample preparation and STM/nc-AFM experiments

The on-surface synthesis experiments were performed under UHV conditions with base pressure below 2×10^{-10} mbar. Au/mica substrates (Phasis) with 200 nm Au layer on top of mica were cleaned by repeated cycles of Ar + sputtering (1 keV) and annealing (470°C) until a clean Au(111) surface was achieved. The precursor molecule 1 was thermally evaporated onto the substrate from quartz crucibles heated at 350°C, which resulted in a deposition rate of ~0.5 Å/min. STM images were acquired with a low-temperature scanning tunneling microscope (Scienta Omicron) operated at 4.7 K in constant-current mode using an etched tungsten tip. Bias voltages are given with respect to the sample. nc-AFM measurements were performed at 4.7 K with a tungsten tip placed on a qPlus tuning fork sensor.[13] The tip was functionalized with a single CO molecule at the tip apex picked up from the previously CO-dosed surface.[14] The sensor was driven at its resonance frequency (25,000 Hz) with a constant amplitude of 70 pm. The frequency shift from resonance of the tuning fork was recorded in constant-height mode using Omicron Matrix electronics and HF2Li PLL by Zurich Instruments. The Δz is positive (negative) when the tip-surface distance is increased (decreased) with respect to the STM set point at which the feedback loop is opened.

4.3 | Computational methods

To compute the DFT band structure of the porous GNR, we used an AiiDAlab[15] app performing gas-phase calculations with the Quantum Espresso[16] software package. We used the Perdew–Burke–Ernzerhof (PBE) exchange-correlation functional.[17] A plane wave basis with an energy cut-off of 400 Ry for the charge density was used together with the projector augmented-wave method (PAW) pseudopotentials (standard solid-state pseudopotentials [SSSP]).[18] A mesh of 26 k-points was used for sampling the 1D Brillouin zone to obtain the electronic ground state. The cell and atomic geometry of the ribbon were relaxed until forces were smaller than 0.001 a.u.

ACKNOWLEDGMENTS

This research was financially supported by the EU Graphene Flagship (Graphene Core 3, 881603), ERC Consolidator Grant (T2DCP, 819698), the Center for Advancing Electronics Dresden (cfaed), the DFG-SNSF Joint Swiss-German Research Project (EnhanTopo, No. 429265950 and 200020_187617) and the Swiss National Science Foundation (Grant No. 200020_182015). The authors acknowledge the use of computational facilities at

the Center for Information Services and High Performance Computing (ZIH) at TU Dresden and at the Swiss Supercomputing Center (CSCS grant s904). Lukas Rotach (Empa) is gratefully acknowledged for technical support during the experiments.

AUTHOR CONTRIBUTIONS

M. R. Ajayakumar: Investigation (equal). **Marco Di Giovannantonio:** Investigation (equal); writing – original draft (equal). **Carlo A. Pignedoli:** Investigation (supporting). **Lin Yang:** Investigation (supporting). **Pascal Ruffieux:** Supervision (supporting); writing – review and editing (supporting). **Ji Ma:** Supervision (equal); writing – original draft (lead). **Roman Fasel:** Supervision (equal); writing – review and editing (equal). **Xinliang Feng:** Supervision (lead); writing – review and editing (equal).

ORCID

M. R. Ajayakumar https://orcid.org/0000-0002-7041-7456
Ji Ma https://orcid.org/0000-0003-4418-2339
Xinliang Feng https://orcid.org/0000-0003-3885-2703

REFERENCES

[1] a) M. Bieri, M. Treier, J. Cai, K. Aït-Mansour, P. Ruffieux, O. Gröning, P. Gröning, M. Kastler, R. Rieger, X. Feng, K. Müllen, R. Fasel, *Chem. Commun.* **2009**, 6919. b) U. Beser, M. Kastler, A. Maghsoumi, M. Wagner, C. Castiglioni, M. Tommasini, A. Narita, X. Feng, K. Müllen, *J. Am. Chem. Soc.* **2016**, *138*, 4322. c) M. Ammon, T. Sander, S. Maier, *J. Am. Chem. Soc.* **2017**, *139*, 12976. d) S. P. Surwade, S. N. Smirnov, I. V. Vlassiouk, R. R. Unocic, G. M. Veith, S. Dai, S. M. Mahurin, *Nat. Nanotechnol.* **2015**, *10*, 459. e) D.-E. Jiang, V. R. Cooper, S. Dai, *Nano Lett.* **2009**, *9*, 4019. f) S. Blankenburg, M. Bieri, R. Fasel, K. Müllen, C. A. Pignedoli, D. Passerone, *Small* **2010**, *6*, 2266. g) J. Yang, M. Ma, L. Li, Y. Zhang, W. Huang, X. Dong, *Nanoscale* **2014**, *6*, 13301. h) A. W. Robertson, G.-D. Lee, K. He, C. Gong, Q. Chen, E. Yoon, A. I. Kirkland, J. H. Warner, *ACS Nano* **2015**, *9*, 11599.

[2] S. P. Koenig, L. Wang, J. Pellegrino, J. S. Bunch, *Nat. Nanotechnol.* **2012**, *7*, 728.

[3] a) C. Moreno, M. Vilas-Varela, B. Kretz, A. Garcia-Lekue, M. V. Costache, M. Paradinas, M. Panighel, G. Ceballos, S. O. Valenzuela, D. Peña, A. Mugarza, *Science* **2018**, *360*, 199. b) P. H. Jacobse, R. D. McCurdy, J. Jiang, D. J. Rizzo, G. Veber, P. Butler, R. Zuzak, S. G. Louie, F. R. Fischer, M. F. Crommie, *J. Am. Chem. Soc.* **2020**, *142*, 13507. c) M. Shekhirev, P. Zahl, A. Sinitskii, *ACS Nano* **2018**, *12*, 8662.

[4] a) R. Pawlak, X. Liu, S. Ninova, P. D'Astolfo, C. Drechsel, S. Sangtarash, R. Häner, S. Decurtins, H. Sadeghi, C. J. Lambert, U. Aschauer, S.-X. Liu, E. Meyer, *J. Am. Chem. Soc.* **2020**, *142*, 12568. b) M. Di Giovannantonio, K. Eimre, A. V. Yakutovich, Q. Chen, S. Mishra, J. I. Urgel, C. A. Pignedoli, P. Ruffieux, K. Müllen, A. Narita, R. Fasel, *J. Am. Chem. Soc.* **2019**, *141*, 12346.

[5] a) A. G. Rajan, K. S. Silmore, J. Swett, A. W. Robertson, J. H. Warner, D. Blankschtein, M. S. Strano, *Nat. Mater.* **2019**, *18*, 129. b) J. C. Buttrick, B. T. King, *Chem. Soc. Rev.* **2017**, *46*, 7. c) J. R. Dias, *J. Phys. Chem. A* **2008**, *112*, 12281. d) J. R. Dias, J.-I. Aihara, *Mol. Phys.* **2009**, *107*, 71.

[6] A. Baskin, P. Král, *Sci. Rep.* **2011**, *1*, 36.

[7] K. Xu, J. I. Urgel, K. Eimre, M. Di Giovannantonio, A. Keerthi, H. Komber, S. Wang, A. Narita, R. Berger, P. Ruffieux, C. A. Pignedoli, J. Liu, K. Müllen, R. Fasel, X. Feng, *J. Am. Chem. Soc.* **2019**, *141*, 7726.

[8] R. Zuzak, I. Pozo, M. Engelund, A. Garcia-Lekue, M. Vilas-Varela, J. M. Alonso, M. Szymonski, E. Guitián, D. Pérez, S. Godlewski, *Chem. Sci.* **2019**, *10*, 10143.

[9] D. J. Rizzo, G. Veber, J. Jiang, R. McCurdy, T. Cao, C. Bronner, T. Chen, S. G. Louie, F. R. Fischer, M. F. Crommie, *Science* **2020**, *369*, 1597.

[10] J. Ma, Y. Fu, J. Liu, X. Feng, *Beilstein J. Org. Chem.* **2020**, *16*, 791.

[11] H. Ito, K. Ozaki, K. Itami, *Angew. Chem. Int. Ed.* **2017**, *56*, 11144.

[12] M. Di Giovannantonio, O. Deniz, J. I. Urgel, R. Widmer, T. Dienel, S. Stolz, C. Sánchez-Sánchez, M. Muntwiler, T. Dumslaff, R. Berger, A. Narita, X. Feng, K. Müllen, P. Ruffieux, R. Fasel, *ACS Nano* **2018**, *12*, 74.

[13] F. J. Giessibl, *Appl. Phys. Lett.* **2000**, *76*, 1470.

[14] L. Bartels, G. Meyer, K.-H. Rieder, D. Velic, E. Knoesel, A. Hotzel, M. Wolf, G. Ertl, *Phys. Rev. Lett.* **1998**, *80*, 2004.

[15] A. V. Yakutovich, K. Eimre, O. Schütt, L. Talirz, C. S. Adorf, C. W. Andersen, E. Ditler, D. Du, D. Passerone, B. Smit, *Comput. Mater. Sci.* **2021**, *188*, 110165.

[16] P. Giannozzi, O. Baseggio, P. Bonfà, D. Brunato, R. Car, I. Carnimeo, C. Cavazzoni, S. d. Gironcoli, P. Delugas, F. F. Ruffino, A. Ferretti, N. Marzari, I. Timrov, A. Urru, S. Baroni, *J. Chem. Phys.* **2020**, *152*, 154105.

[17] J. P. Perdew, K. Burke, M. Ernzerhof, *Phys. Rev. Lett.* **1996**, *77*, 3865.

[18] K. Lejaeghere, G. Bihlmayer, T. Björkman, P. Blaha, S. Blügel, V. Blum, D. Caliste, I. E. Castelli, S. J. Clark, A. Dal Corso, *Science* **2016**, *351*, 351.

SUPPORTING INFORMATION

Additional supporting information may be found in the online version of the article at the publisher's website.

How to cite this article: M. R. Ajayakumar, M. Di Giovannantonio, C. A. Pignedoli, L. Yang, P. Ruffieux, J. Ma, R. Fasel, X. Feng, *J. Polym. Sci.* **2022**, 1. https://doi.org/10.1002/pol.20220003